for $j = 1$ to m' do
$S_j \leftarrow M_j \odot I_i$;
$c_j = \Sigma_{i=1}^{r} s_{ji}$;
Step 2:
find S_k $(1 \le k \le m')$ such that
$c_k = \min\{c_1, c_2, ..., c_{m'}\}$;
$min\_set \leftarrow S_k$;
$mid\_switch \leftarrow mid\_switch \cup \{k\}$;
if $min\_set \neq \phi$ then
for $j = 1$ to m' do
$S_j \leftarrow S_j \cap min\_set$
until $min\_set = \phi$;
Step 3:
connect I_i through the middle switches in *min_switch* and update the destination sets of these middle switches.
End

Conclusion: In ATM networks, a call should be set up within a short time. However, the CAC mechanism needs to check each link and node along the path to decide if a call can be accepted. This may lead to an unacceptable call setup delay since there may be many internal links between a pair of input-output port within a switch. If the CAC mechanism only needs to check the status of external ports, the call setup time can be reduced. In this Letter, a wide-sense non-blocking multicast ATM switch is designed, based on the Clos network. Using this switch, the external link utilisation is very high. By the path-establishing algorithm presented here, the number of required middle stage switches is significantly reduced, compared with the number required in strictly non-blocking multicast switches.

© IEE 1997
28 January 1997
Electronics Letters Online No: 19970318

K.S. Chan, S. Chan and K.L. Yeung (*Department of Electronic Engineering, City University of Hong Kong, Tat Chee Avenue, Kowloon, Hong Kong*)

References

1 CLOS, C.: 'A study of non-blocking switching networks', *Bell Syst. Tech. J.*, 1953, **32**, pp. 406–424
2 MELEN, R., and TURNER, J.S.: 'Nonblocking multirate distribution networks', *IEEE Trans. Commun.*, 1993, **41**, pp. 362–369
3 SVINNSET, I.: 'Nonblocking ATM switching networks', *IEEE Trans. Commun.*, February/March/April 1994, **42**, pp. 1352–1358
4 TURNER, J.S.: 'An optimal nonblocking multicast virtual circuit switch'. Proc. INFO-COM'94, 1994, pp. 298–305
5 YANG, Y., and MASSON, G.M.: 'Nonblocking broadcast switching networks', *IEEE Trans. Comput.*, 1991, **40**, pp. 1005–1015

Special purpose hardware for time frequency analysis

D. Petranović, S. Stanković and L.J. Stanković

Indexing terms: Time-frequency analysis, Computer architecture

A special purpose hardware system for time-frequency signal analysis is presented. This system is based on the S-method which has the significant advantage of using the short time Fourier transform as an intermediate step in its implementation. The hardware designed for a fixed point arithmetic is well-structured and suitable for VLSI implementation. An example including an error analysis is also provided.

Introduction: Time-frequency signal analysis is used for signals whose frequency changes with time, in applications where a time distribution of frequency content is of interest. The important applications, among others, include radar, sonar, seismic and speech signal analysis, [1]. The short time Fourier transform (STFT) is the simplest tool for time-frequency analysis, and has been conventionally used for that purpose. However, its serious disadvantage is low concentration in the time-frequency plane which may be inconvenient in many applications. Various quadratic distributions, the most important of which is the Wigner distribution, have been used to improve the resolution, [2, 3]. The Wigner distribution generally gives a better concentration than the STFT, but it produces cross-terms in case of multicomponent signals which limits its applicability. Significant research and effort has been made to reduce the cross-terms effects [2, 3]. The recently proposed S-method [4 – 7] reduces or completely eliminates cross-terms without sacrificing the high resolution of Wigner distribution. In addition, it establishes a clear relationship with the STFT, which has been well studied and understood and has been used for many years.

Increasing demands for high speed real time applications of the time-frequency analysis require an efficient hardware implementations of developed algorithms. The fact that the S-method uses the STFT as an intermediate step, for which the hardware implementations already exist, makes this method very attractive for implementation. In this Letter we present an architecture and hardware design for VLSI implementation of S-method. For efficient ASIC implementation, complete hardware for the S-method based algorithm, which includes the STFT implementation, has been developed.

Review of S-method: The short-time Fourier transform (STFT) in a discrete form is given by [2 – 5, 11, 12, 14, 15]

$$STFT(n,k) = \sum_{i=-N/2+1}^{N/2} f(n+i)w(i)e^{-j\frac{2\pi}{N}ik} \quad (1)$$

The Wigner distribution (WD) in the discrete domain is defined by [2, 3]:

$$WD(n,k) = \sum_{i=-N/2+1}^{N/2} f(n+i)f^*(n-i)w(i)w(-i)e^{-j\frac{2\pi}{N}2ik} \quad (2)$$

where $w(i)$ is a real window. Based on the relationship between STFT and WD, established in [4], the S-method is derived as:

$$SM(n,k) = SPEC(n,k) + 2\sum_{i=1}^{L_d} \mathrm{Re}\{STFT(n,k+i)STFT^*(n,k-i)\} \quad (3)$$

where L_d is a width of the rectangular frequency domain window. Denoted by $SPEC(n, k)$ is the squared modulus of the STFT called the spectrogram. Through a suitable selection of the window width (L_d), it is possible to obtain the auto-terms of multicomponent signals such that they remain unchanged with respect to the WD, while the entire elimination (or reduction) of cross-terms is achieved (more details on this window may be found in [4 – 9]). It can be observed that: (i) for $L_d = 0$ we get the SPEC, and (ii) for $L_d = N/2$ the WD follows (in this case the last summation term should be divided by 2).

Implementation: In this Section, we present a system for the S-method implementation. The proposed architecture consists of two blocks. The first block is used for the STFT implementation and the second block is used to modify the STFT in order to obtain the improved distribution based on the S-method. The STFT can be implemented using available FFT chips or the approaches based on the recursive algorithms. The design presented here is based on the recursive algorithm [4, 11, 12] which is, due to reduced hardware complexity, more suitable for VLSI implementation. Assuming a rectangular window $w(i)$ the STFT can be written as:

$$STFT(n,k) = [f(n+N/2) - f(n-N/2)](-1)^k + STFT(n-1,k)e^{j2\pi k/N} \quad (4)$$

A complete system consists of N channels described by eqn. 4, with $k = 0, 1, 2, ... N-1$. For the cases of a Hanning or Hamming window $w(i)$, the short time Fourier transform is obtained by modifying $STFT(n, k)$ in eqn. 4 as $STFT_H(n, k) = a_{-1}STFT(n, k-1) + a_0STFT(n, k) + a_1STFT(n, k+1)$, where the coefficients a_{-1}, a_0, a_1

are: (0.25, 0.5, 0.25) or (0.23, 0.54, 0.23) for the Hanning or the Hamming window, respectively [4, 5, 12].

Each channel described by eqn. 4, involves complex multiplication and can be separated in two sub-channels involving only real computations. To describe these channels, we modify eqn. 4, separating real and imaginary parts into two sub-channels as:

$$\begin{aligned} STFT_{Re}(n,k) &= F(n)(-1)^k + c(k)STFT_{Re}(n-1,k) \\ &\quad - s(k)STFT_{Im}(n-1,k) \\ STFT_{Im}(n,k) &= c(k)STFT_{Im}(n-1,k) \\ &\quad + s(k)STFT_{Re}(n-1,k) \end{aligned} \tag{5}$$

where $STFT_{Re}(n, k)$ and $STFT_{Im}(n, k)$ are the real and imaginary parts in $STFT(n, k)$, respectively, and $c(k) = \cos(2\pi k/N)$; $s(k) = \sin(2\pi k/N)$; $F(n) = f(n + N/2) - f(n - N/2)$. Now, eqn. 3 can be written as:

$$\begin{aligned} SM(n,k) &= |STFT(n,k)|^2 \\ &\quad + 2\sum_{i=1}^{L_d} STFT_{Re}(n,k+i)STFT_{Re}(n,k-i) \\ &\quad + 2\sum_{i=1}^{L_d} STFT_{Im}(n,k+i)STFT_{Im}(n,k-i) \end{aligned} \tag{6}$$

which is the equation used to modify the outputs of STFT block in order to obtain the S-method based distribution.

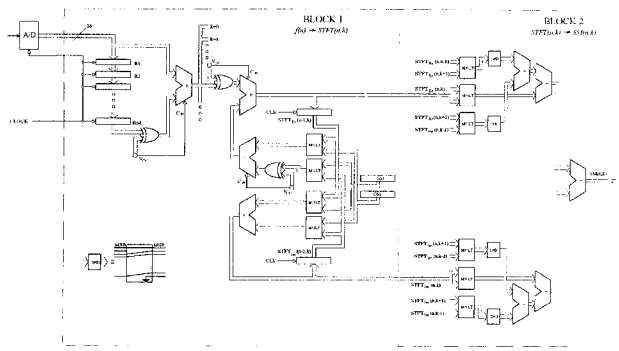

Fig. 1 *Hardware for S-method realisation (one channel with $L_d = 2$)*

The hardware necessary for one channel implementation (with $L_d = 2$) is presented in Fig. 1. It has been designed for a 16-bit fixed-point-arithmetic. The total number of multipliers is $2(L_d+3)$ and the total number of adders is $2(L_d+2)$. The multiplication operation results in two-sign-bit and, assuming Q15 format (15 fractional bits), the product mast be shifted left by one bit to obtain correct results. This shifter is included as a part of multiplier. The throughput of the system is N. The longest path is the one that connects the register storing $STFT(n-1, k\pm L_d)$, through two multipliers and L_d+3 adders, with the output $SM(n, k)$. This path determines the fastest sampling rate. It can be observed that the S-method implementation introduces only an additional delay of L_d adders compared to the spectrogram implementation. Thus the fastest sampling rate is essentially the same for both implementations. This design can be implemented as an ASIC chip to meet the speed and performance demands of very fast real time applications.

Error analysis and example: The use of finite word length registers in the implementation introduces two types of errors: a signal quantisation error and a multiplication error. It is assumed that the signal is properly scaled to avoid an overflow. The quantisation error can be modelled by an input additive noise. In this case we have $f(n) + \epsilon(n)$ at the input instead of $f(n)$. Mathematically this reduces to a well known situation of noisy signal [9, 13] with distribution variance

$$\sigma^2 = \frac{N^2\sigma_\epsilon^4}{2L_d+1} + \frac{N\sigma_\epsilon^2}{(2L_d+1)^2}\sum_{i=-L_d}^{L_d} SPEC_f(n,k+i) \tag{7}$$

where $\sigma_\epsilon^2 = 2^{-2b}/12$ is the quantisation noise variance [10]. Note that for spectrograms of order 1 and $N\sigma_\epsilon^2 \ll 1$, this expression is of order $N\sigma_\epsilon^2/(2^{-2b} + 1)^2 = N2^{-2b}/(12(2L_d + 1)^2)$. For example, for $N = 64$, $b = 16$ and $L_d = 2$, $_s^2$ is of order 2^{-34}.

The multiplication error $q(n)$ due to the quantisation of product $STFT(n-1, k)e^{j2\pi k/N}$, in eqn. 4, has the variance $\sigma_q^2 = 2^{-2b}/4$ [10]. This error accumulates with each iteration. After M iterations its variance is of order $M\sigma_q^2$. For extremely large signal sequences (for our example, with $b = 16$, large M means $M > 10^9$) we have to use either hardware with wider registers or we need to compensate for the accumulation error. Note that the proposed two-block solution has built in flexibility, which allows us to use any available hardware for the Fourier transform realisation. Namely, the first block for the STFT calculation (Fig. 1) can be implemented with the FFT based algorithms, instead of the recursive one. In that case, the accumulation error would be avoided and kept in the order as in eqn. 7.

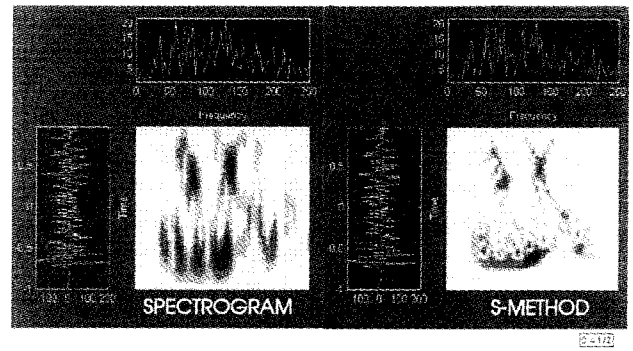

Fig. 2 *Time-frequency analysis of seismic signal*
a Spectrogram, *b* S-method with $L_d = 2$

The proposed architecture is simulated with 16-bit registers on a real seismic signal. The results obtained with the spectrogram and the S-method are presented in Fig. 2. It can be seen that the concentration improvement is high for a very small $L_d = 2$.

Conclusion: Special purpose hardware has been designed to implement the S-method based algorithm for time frequency signal analysis. The hardware is well structured and suitable for VLSI implementation and can be run with a clock of essentially the same frequency as the one for the spectrogram implementation system. The error analysis, which can be used for appropriate hardware selection, is presented.

© IEE 1997
23 January 1997
Electronics Letters Online No: 19970361

D. Petranović, S. Stankovic and L.J. Stanković (*Elektrotehnicki fakultet, 81000 Podgorica, Montenegro, Yugoslavia*)

E-mail: l.stankovic@ieee.org

References

1 Proceeding of the IEEE special issue 'Time frequency analysis', 1996, **84**, (9)
2 COHEN, L.: 'Time-frequency distributions - a review', *Proc. IEEE*, 1989, **77**, pp. 941–981
3 HLAWATSCH, F., and BROUDREAUX-BARTELS, G.F.: 'Linear and quadratic time-frequency signal representation', *IEEE SP Mag.*, April 1992, pp. 21–67
4 STANKOVIĆ, L.J.: 'A method for time-frequency analysis', *IEEE Trans. SP*, 1994, **42**, pp. 225–229
5 STANKOVIĆ, L.J.: 'An analysis of some time-frequency and time-scale distributions', *Annales des Telecomm.*, 1994, **9/10**, pp. 505–517
6 STANKOVIĆ, L.J.: 'A multitime definition of the Wigner higher order distribution: L-Wigner distribution', *IEEE SP Lett.*, 1994, **1**, (7), pp. 106–109
7 STANKOVIĆ, L.J.: 'A method for improved energy concentration in the time-frequency signal analysis using the L-Wigner distribution', *IEEE Trans. SP*, 1995, **5**, (43), pp. 1262–1268
8 STANKOVIĆ, S., STANKOVIĆ, L.J., and USKOKOVIĆ, Z.: 'On the local frequency, group shift and cross-terms in the multidimensional time-frequency distributions; A method for multidimensional time-frequency analysis', *IEEE Trans. SP*, 1995, **43**, (7), pp. 1719–1725
9 STANKOVIĆ, L.J., IVANOVIĆ, V., and PETROVIĆ, Z.: 'Unified approach to the noise analysis in the Wigner distribution and spectrogram', *Annales des Telecomm.*, (in print)

10 OPPENHEIM, A., and SCHAFER, R.: 'Digital signal processing' (Prentice-Hall, Englewood Cliffs, NJ, 1975)
11 PAPOULIS, A.: 'Signal analysis' (McGraw-Hill Book Company, 1977)
12 LIU, K.J.R.: 'Novel parallel architectures for short-time Fourier transform', *IEEE Trans. CAS*, 1993, **40**, (12), pp. 786–789
13 STANKOVIĆ, L.J., and STANKOVIĆ, S.: 'On the Wigner distribution of discrete-time noisy signals with application to the study of quantization effect', *IEEE Trans. SP*, 1994, **42**, pp. 1863–1867
14 AMIN, M.G.: 'A new approach to recursive Fourier transform', *Proc. IEEE*, 1987, **75**, pp. 1537
15 UNSER, M.: 'Recursion in short time signal analysis', *Sig. Process.*, 1983, **5**, pp. 229–240

Iterative boundary condition (IBC) in finite difference solving scattering problems of open region

Luo Yong-Lun and Luk Kwai-Man

Indexing terms: Numerical methods, Finite difference methods, Electromagnetic wave scatter

A novel truncation boundary condition, the iterative boundary condition (IBC), is proposed for finite difference (FD) solving electromagnetic scattering problems. The iterative process of this condition is given. Solutions of the IBC for some 2D cylinder scattering problems have been obtained and are compared with solutions using MoM [1] and MEI [2]. These solutions show very good agreement.

Introduction: The FD method is a basic method for electromagnetic scattering problems. A proper truncation boundary condition must be addressed for the exterior layer nodes. In the past, ABC [3] and MEI [2] have been successfully applied as a FD mesh truncation method. In this Letter, we present the concept of IBC to truncate the FD mesh layer. This novel truncation boundary condition is expressed by an equation of fields at the exterior layer node and its immediately inner layer node. An iterative process is used to find the IBC coefficient and solution of the scattering problem.

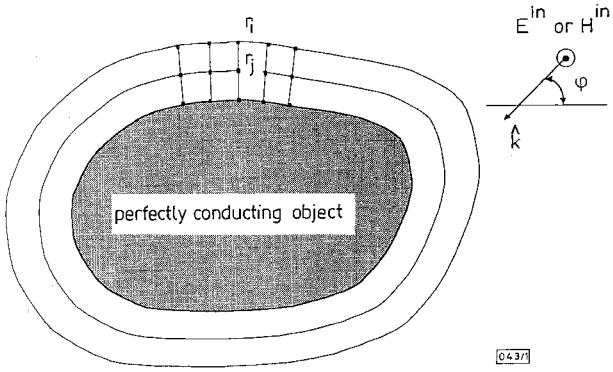

Fig. 1 *Conformal FD mesh for IBC recipe*

Theory: Consider the electromagnetic scattering problem of a 2D perfectly conducting object, as shown in Fig. 1. The FD method is used to calculate the scattered field of this problem. A conformal mesh is generated. Let the surface induced current be $J(\vec{r}')$. Node $\vec{r}_i$ is on the exterior mesh layer and node $\vec{r}_j$ is the immediate inner node of $\vec{r}_i$. Let the scattered scalar fields at these two nodes be $\phi(\vec{r}_i)$ and $\phi(\vec{r}_j)$. For these two fields, we can find a coefficient $A(\phi(\vec{r}_i), \phi(\vec{r}_j))$ which satisfies

$$\Phi(\vec{r}_i) + A(\vec{r}_i, \vec{r}_j)\Phi(\vec{r}_j) = 0 \qquad (1)$$

or

$$A(\vec{r}_i, \vec{r}_j) = -\frac{\Phi(\vec{r}_i)}{\Phi(\vec{r}_j)} \qquad (2)$$

where $\phi(\vec{r}_i) = \oint_{c_0} J(\vec{r}')G(\vec{r}, \vec{r}')dl'$, c_0 is the cross-section boundary of the cylinder and $G(\vec{r}, \vec{r}')$ is the Green function. Eqns. 1 and 2 are the field equations of these two nodes. $A(\vec{r}_i, \vec{r}_j)$ is a coefficient that not only exactly reflects the field relation of $\phi(\vec{r}_i)$ and $\phi(\vec{r}_j)$, but also embodies the information of location, object geometry and induced current source.

To obtain $A(\vec{r}_i, \vec{r}_j)$ for all nodes ($i = 1, 2, ..., N$) on the exterior layer, an iterative process is used. N is the total number of nodes on the exterior layer. The process of IBC starts with setting an initial trial current $J^0(\vec{r}')$ on the conducting surface. The field radiated by $J^0(\vec{r}')$ at node $\vec{r}_i$ is made to be related to the field at its immediate inner node $\vec{r}_j$ by eqn. 1. $A(\vec{r}_i, \vec{r}_j)$ is calculated from eqn. 2. $A(\vec{r}_i, \vec{r}_j)$ is used as the newer field relation coefficient or truncation BC for the exterior layer nodes. We simulate the new field value $\Phi^1(\vec{r}_i)$ for node $\vec{r}_i$ from eqn. 1 as:

$$\Phi^1(\vec{r}_i) + A(\vec{r}_i, \vec{r}_j)\Phi^1(\vec{r}_j) = 0 \qquad (3)$$

By applying FD equations of interior mesh nodes, a sparse equation for the whole scattering problem is then set up. By solving this sparse equation, the scattered fields at all mesh nodes are obtained. Using these field values, a new value of induced current $J^1(\vec{r}')$ could therefore be calculated.

Using $J^1(\vec{r}')$ as the new trial current and repeating the above process iteratively, steady solutions for $A(\vec{r}_i, \vec{r}_j)$, $\phi(\vec{r}_i)$ and $J(\vec{r}')$ can finally be obtained. The termination of the iterative process depends on the accuracy needed. To obtain as accurate solutions as possible for $J(\vec{r}')$ or $\phi(\vec{r}_i)$, the solution of $A(\phi(\vec{r}_1), \phi(\vec{r}_2)$ must be as accurate as possible. It should be made clear that eqns. 1 and 2 are not an artificially truncated BC for terminating FD mesh layers. Theoretically, eqns. 1 and 2 are exact field relation equations and no approximation has been made to these equations. The calculation error is mainly due to the numerical integral, except the intrinsic error of the FD method.

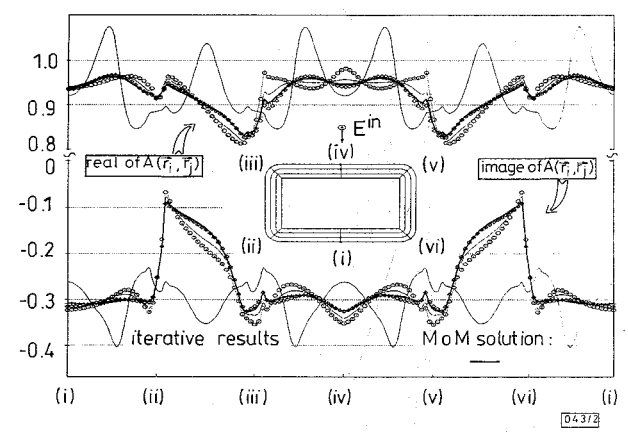

Fig. 2 *Convergence of IBC solutions for 2D rectangular cylinder scatterer with $A(\vec{r}_i, \vec{r}_j)$*

$1\lambda \times 2\lambda$ and $\varphi = 0°$
Incident wave is TM wave
——— 1st, O 2nd, – – – – 3rd, ◇ 4th, + 5th

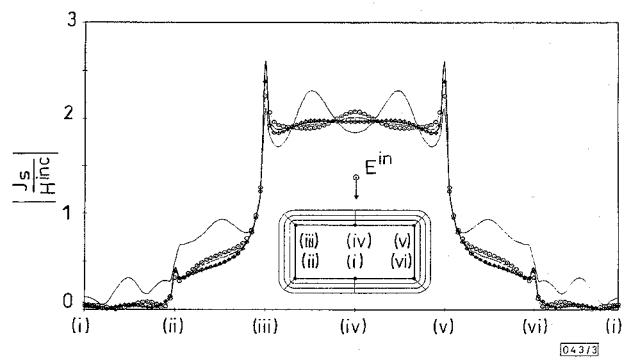

Fig. 3 *Convergence of IBC solutions for 2D rectangular cylinder scatterer with induced current $J(\vec{r}')$*

$1\lambda \times 2\lambda$ and $\varphi = 0°$
Incident wave is TM wave
——— 1st, O2nd, – – – – 3rd, ◇ 4th, + 5th,
——— MoM solution